Future Technology
Open Access Journal
ISSN 2832-0379

August 2026| Volume 05 | Issue 03 | Pages 97-106

Journal homepage: https://fupubco.com/futech

https://doi.org/10.55670/fpll.futech.5.3.9

Future Publishing LLC

Article

Federated leveraging AI-assisted MPPT for real-time photovoltaic performance optimization using machine learning

Srinivas S[1]*, Shamala N[2], Yogesh T[3]

[1]Department of Electronics and Communication Engineering, VTU PG Centre, Mysuru, India
[2]Department of Electrical and Electronics, VVIET, Mysuru, India
[3]Department of Computer Science & Engineering, VTU PG Centre Mysuru, Karnataka, India

ARTICLE INFO

Article history:
Received 22 November 2025
Received in revised form
24 March 2026
Accepted 05 May 2026

Keywords:
Photovoltaic systems, AI-assisted control,
Maximum power point tracking,
Incremental Conductance

*Corresponding author
Email address:
Srinivas.s043@gmail.com

DOI: 10.55670/fpll.futech.5.3.9

ABSTRACT

Maximum power point tracking is a necessary power optimization technique for maximizing the energy output of photovoltaic PV systems that operate in variable environmental conditions. While classical MPPT algorithms, such as Perturb and Observe and Incremental Conductance (IncCond), are well implemented, research is now underway on artificial intelligence techniques to improve tracking performance. This paper reports on a control-oriented benchmarking study of classical and AI-assisted MPPT strategies within a unified discrete-time simulation framework implemented in MATLAB. An artificial neural network is proposed in an AI-assisted MPPT architecture to estimate the optimal PV operating voltage, while a conventional proportional-integral voltage controller enforces it and maintains closed-loop stability. The performance of P&O, IncCond, and the AI-assisted MPPT is studied under uniform irradiance steps, fast irradiance fluctuations, and partial shading conditions. Under a 1000->600 W/m^2 irradiance step, IncCond delivers a tracking efficiency of 99.89% with very low power ripple (0.0014 W), which is significantly better than P&O (98.13%) and the AI-assisted approach (67.92%). In partial shading, P&O and IncCond have efficiencies of 96.21% and 92.99%, respectively, while the AI-assisted MPPT has an efficiency of 67.84%. These results show that the IncCond is a strong and reliable baseline, and that the AI-assisted MPPT offers valuable insight into hybrid control design and requires careful, control-aware integration.

1. Introduction

Photovoltaic (PV) energy conversion systems exhibit inherently nonlinear current-voltage (I-V) and power-voltage (P-V) characteristics, and their maximum power point (MPP) varies continuously with solar irradiance and cell temperature. In practical installations, environmental conditions change unpredictably because of cloud transients, thermal variations, and partial shading. As a result, PV modules may operate away from their optimal point unless an appropriate control strategy is applied. Maximum power point tracking (MPPT) is therefore essential for maximizing energy extraction and ensuring efficient and reliable PV operation, particularly under dynamic conditions. Conventional MPPT algorithms such as Perturb and Observe (P&O) and Incremental Conductance (IncCond) remain widely used because of their simplicity and modest computational requirements. However, both methods have inherent limitations. P&O relies on iterative perturbations of the operating point and therefore introduces unavoidable steady-state oscillations, with degraded performance under rapidly changing irradiance. IncCond improves tracking by explicitly evaluating the slope of the P-V characteristic, enabling more accurate convergence under slowly varying conditions. Nevertheless, IncCond can still be affected by noise in measurements and derivative estimation errors, and its performance may degrade under rapid environmental changes or partial shading, where multiple local maxima may appear on the P-V curve. The increasing integration of PV systems into smart grids and distributed energy networks has stimulated interest in more advanced MPPT methods that can better handle nonlinearities and uncertainty. In this context, artificial intelligence (AI) and machine learning (ML) have emerged as promising approaches because they can approximate nonlinear mappings directly from data without requiring fully explicit analytical models. Hoang et al. [1] reported the use of AI-based prediction of MPP voltage and

current to reduce sensing requirements and system complexity, while Zečević and Rolevski [2] demonstrated the use of neural networks for irradiance estimation and MPPT-related prediction. A variety of intelligent MPPT approaches have since been investigated. Du et al. [3] proposed a fuzzy-weighted extreme learning machine to improve adaptability under varying operating conditions, and Chou et al. [4] studied reinforcement learning for MPPT through interaction-based policy learning. Although such approaches may deliver strong performance, they often replace classical control logic entirely, raising concerns about stability guarantees, interpretability, and real-time deployability. ANN-based MPPT methods remain particularly popular, and Khan and Mathew [5] and Xie and Wu [6] reported improved tracking accuracy through data-driven estimation. However, much of the existing AI-MPPT literature focuses on prediction accuracy or energy gain without sufficiently examining the interaction between the learning component and the closed-loop control structure.

A common implicit assumption in many AI-driven MPPT studies is that better prediction accuracy will automatically lead to better control performance. This assumption does not always hold in systems with fast dynamics, multi-timescale control layers, and actuator constraints. Therefore, there is a clear need for control-oriented studies that critically evaluate the integration of AI within classical MPPT architectures, rather than treating AI as a wholesale replacement for conventional control logic. To address this gap, the present work investigates an AI-assisted MPPT framework in which machine learning is used strictly as a supporting estimation component. An artificial neural network is employed to predict the optimal PV operating voltage at the MPP, while a conventional proportional-integral (PI) voltage controller enforces this reference via a DC-DC boost converter. This hybrid architecture preserves the classical control structure and enables transparent benchmarking against P&O and IncCond. The main objectives of this study are as follows:

- To develop an ANN-based MPPT framework for estimating the optimal PV operating voltage and integrating it into a conventional closed-loop voltage-control architecture.
- To perform a control-oriented comparative evaluation of P&O, IncCond, and AI-assisted MPPT under dynamic irradiance and partial-shading conditions.
- To analyze the robustness, limitations, and integration challenges of AI-assisted MPPT relative to established classical methods.

2. Literature review

Maximum power point tracking (MPPT) is still one of the main challenges in photovoltaic (PV) energy conversion because of the nonlinearity in the current voltage and power and voltage characteristics and their strong dependence on irradiance and temperature. Conventional MPPT techniques such as Perturb and Observe (P&O) and Incremental Conductance (IncCond) continue to dominate industrial applications due to the low computational cost of these simple methods. However, these techniques have their own limitations, including steady-state oscillations, sensitivity to measurement noise, and reduced robustness to partial shading and rapid environmental changes. These shortcomings have led to extensive research into advanced MPPT strategies that better handle nonlinearities and operational uncertainties. Artificial intelligence (AI)-based approaches have become of interest as promising alternatives to classical MPPT methods, especially in complex operating scenarios. Bouaouaou et al. [7] presented a combined model predictive control and ANN-based MPPT strategy for multilevel grid-connected PV inverters and demonstrated enhanced regulatory performance but also increased computational complexity and implementation burden. Reinforcement learning has been investigated as a data-driven control paradigm that does not require explicit system modeling. Avila et al. [8] proposed a deep reinforcement learning-based MPPT controller for partially shaded PV systems, enabling global maximum power point tracking through trial-and-error learning. Giraldo et al. [9] further developed this direction by experimentally verifying a global MPPT strategy based on a deep Q-network in real PV systems, showing that learning-based controllers can outperform classical methods under certain conditions; however, they pose challenges for training stability and real-time safety.

In MPPT, recent studies have focused on the importance of temporal learning and predictive capability. Wadehra et al. [10] used deep recurrent reinforcement learning to model time-dependent changes in irradiance and achieved better tracking performance under fast-changing conditions. Yin et al. [11] proposed a deep predictive data representation model control framework for MPPT under partial shading conditions and proved that performance improvement is not only related to prediction accuracy but also to the close coupling between the learning model and the control logic. These results indicate that the success of MPPT in artificial intelligence depends heavily on how learning components are incorporated into the control architecture.

Hybrid intelligent approaches have also been sought to balance adaptability and interpretability. Danyali et al. [12] proposed a neuro-fuzzy MPPT for grid-connected PV systems under partial shading, which is more robust while retaining the rule-based transparency. Wang et al. [13] proposed a hybrid perturb-and-observe-based MPPT strategy that combines multiple heuristics to enhance global tracking capability, demonstrating that incremental changes to classical methods can yield performance benefits without entirely replacing the existing control logic. Chnini et al. [14] emphasized the importance of implementation realism and therefore validated ANFIS-based MPPT strategies using processor-in-the-loop contributions that highlighted computation constraints and the real-time feasibility of intelligent MPPT deployment. Besides direct MPPT control, machine learning has other applications for the broader optimization of PV performance, such as regression-based estimation of the MPP voltage or power. Satpathy et al. [15] proposed an online deep ridge extreme learning machine for real-time MPPT in PV-based microgrids, showing that online adaptation can address the issue of distribution shift, thereby adding complexity in terms of stability and computational burden.

Despite good progress, a critical reading of the literature shows that many MPPT studies based on artificial intelligence (AI) aim to increase prediction accuracy and/or energy gain without thoroughly analyzing the closed-loop control interaction, stability margins, and supervisory timing effect. Moreover, a considerable part of the existing work consists of completely replacing classical MPPT logic, which limits transparency and makes it difficult to benchmark fairly. Only a few studies explicitly consider integrating ANN-based MPP estimation with real-time voltage regulation within a conventional control structure. This gap motivates the present work, which is based on a control-oriented artificial intelligence (AI)- assisted MPPT framework to critically assess the role of machine learning as a supporting estimator rather than as a controlling authority.

3. System modeling and methodology

This section presents a control-oriented PV boost-converter framework for comparing P&O, Incremental Conductance (IncCond), and an AI-assisted MPPT strategy. In the proposed framework, the AI component is restricted to estimating the MPP voltage, while a conventional PI controller enforces the operating point. This structure enables fair benchmarking, stable operation, and rigorous evaluation under common modeling and simulation conditions. The overall design and signal flow of the proposed AI-assisted MPPT framework, including the plant dynamics, measurement, control, and benchmarking layers, are shown in Figure 1.

3.1 Overall system architecture

The investigated photovoltaic (PV) energy conversion system consists of a PV array interfaced with a DC-DC boost converter and controlled by a maximum power point tracking (MPPT) layer. Three MPPT strategies are evaluated within the same simulation framework: Perturb and Observe (P&O), Incremental Conductance (IncCond), and an AI-assisted MPPT strategy. An inner proportional-integral (PI) voltage-control loop regulates the PV operating voltage by adjusting the converter duty cycle. A key feature of the proposed framework is the separation of MPP estimation from actuator-level control. In conventional MPPT methods, the duty cycle or voltage reference is directly perturbed during the search process. In contrast, the AI-assisted method separates the estimation of the optimal operating point from its enforcement. The artificial neural network (ANN) is used only to estimate the PV voltage at the maximum power point, while the PI controller ensures stable, physically realizable tracking through the power converter. This structure preserves the conventional control hierarchy and allows transparent benchmarking against classical MPPT method.

3.2 Photovoltaic and converter modeling

The PV array is modeled using a datasheet-based single-diode model representative of a 1 kW-class system. The module current is described by:

$$I = I_{ph} - I_o\left[\exp\left(\frac{V+IR_s}{nV_t}\right) - 1\right] - \frac{V+IR_s}{R_{sh}} \quad (1)$$

where $I$and $V$are the module current and voltage, $I_{ph}$is the photocurrent, $I_o$is the diode reverse saturation current, $R_s$and $R_{sh}$are the series and shunt resistances, $n$is the diode ideality factor, and the thermal voltage is $V_t = N_{s,cell}kT/q$. The photocurrent is adjusted according to irradiance and temperature as:

$$I_{ph} = \left(\frac{G}{G_{ref}}\right)\left[I_{sc,ref} + \alpha_{Isc}(T - T_{ref})\right] \quad (2)$$

where $G_{ref} = 1000\ W/\text{m}^2$and $T_{ref} = 298.15$. The reverse saturation current is updated with temperature using:

$$I_o(T) = I_{o,ref}\left(\frac{T}{T_{ref}}\right)^3 \exp\left[\frac{E_g q}{nk}\left(\frac{1}{T_{ref}} - \frac{1}{T}\right)\right] \quad (3)$$

which is consistent with the implemented MATLAB model. At the array level, the system uses 4 modules in series and 1 string in parallel, giving an MPP voltage close to 120 V under standard test conditions. The implicit PV current equation in (1) is solved numerically using a Newton-based iterative method for each operating point. This same model is used for uniform-irradiance and partial-shading simulations, with module-level irradiance mismatch introduced during shaded cases to generate the required I-V and P-V characteristics. PV model parameters are also shown in Table 1.

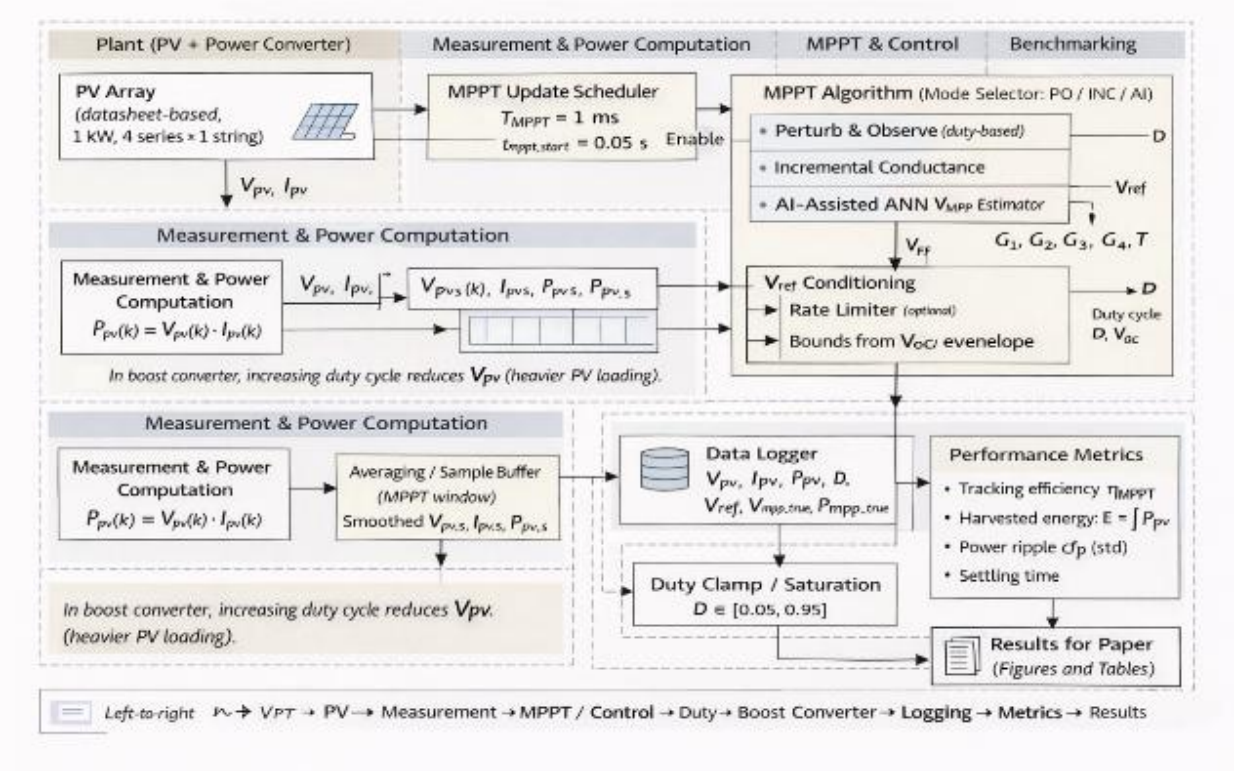

Figure 1. Block diagram of the AI-assisted MPPT framework for photovoltaic system benchmarking

Table 1. PV module and model parameters

Parameter	Symbol	Value
Electron charge	(q)	(1.602176634 \times 10^{-19}) C
Boltzmann constant	(k)	(1.380649 \times 10^{-23}) J/K
Reference irradiance	(G_{ref})	1000 W/m(^2)
Reference temperature	(T_{ref})	298.15 K
Cells in series per module	(N_{s,cell})	60
Open-circuit voltage at STC	(V_{oc,ref})	37.2 V
Short-circuit current at STC	(I_{sc,ref})	8.87 A
Diode ideality factor	(n)	1.3
Series resistance	(R_s)	0.35 (\Omega)
Shunt resistance	(R_{sh})	1000 (\Omega)
Silicon bandgap energy	(E_g)	1.12 eV
Current temperature coefficient	(\alpha_{Isc})	(0.0005 I_{sc,ref}) A/K
Voltage temperature coefficient	(\beta_{Voc})	(-0.0023 V_{oc,ref}) V/K

The power-conditioning stage is modeled as an averaged boost converter operating in continuous-conduction mode. The converter states are the inductor current $i_L$and the output capacitor voltage V_{dc}. The corresponding averaged state equations are given by (4) and (5):

$$\frac{di_L}{dt} = \frac{V_{pv}-(1-D)V_{dc}}{L} \quad (4)$$

$$\frac{dV_{dc}}{dt} = \frac{(1-D)i_L-\frac{V_{dc}}{R_{load}}}{C} \quad (5)$$

For digital simulation, the model is discretized using a forward-Euler update with a sampling time T_s, as expressed in (6):

$$x(k+1) = x(k) + T_s\dot{x}(k) \quad (6)$$

where $L = 2\,\text{mH}$, $C = 1000\,\mu\text{F}$, $T_s = 100\,\mu\text{s}$, and $0.05 \le D \le 0.95$.

An inner PI voltage controller regulates the PV operating voltage by generating the converter duty cycle from the error

$$e(k) = V_{pv}(k) - V_{ref}(k) \quad (7)$$

The implemented gains are $K_p = 0.006$and $K_i = 8.0$, with $T_s = 100$us. To improve robustness, the controller uses a filtered PV-voltage signal, duty-rate limiting, integrator clamping, conditional anti-windup, and integrator reset for large reference changes. The PI gains were tuned manually via iterative simulation to achieve a stable voltage response with minimal overshoot and a settling time below 10 ms in response to step changes in irradiance. The chosen values provided a good balance between tracking speed and robustness against measurement noise. All controllers are implemented in discrete time, with the plant dynamics updated at a fixed integration step and the MPPT algorithms executed at a slower supervisory sampling rate. This structure reflects the practical implementation of digital control and enables consistent comparison across all MPPT strategies.

3.3 Classical MPPT benchmarks

Two widely used classical MPPT algorithms are employed as benchmark controllers. The P&O method directly updates the converter duty cycle. A fixed perturbation step $\Delta D = 0.0015$ is applied in each MPPT cycle, and the resulting change in PV power determines whether to continue in the same direction or reverse direction. Although simple and easy to implement, this method introduces steady-state oscillations around the maximum power point and may converge slowly under rapidly varying irradiance. In the implemented benchmark, the P&O method updates the operating reference once per MPPT cycle using a fixed perturbation step, so the observed steady-state ripple is directly related to the perturbation mechanism and the supervisory update rate. The Incremental Conductance (IncCond) method exploits the relation between incremental conductance and instantaneous conductance at the maximum power point. By explicitly using the slope of the P-V characteristic, IncCond provides more accurate steady-state tracking and greater robustness under varying environmental conditions. These properties make it a strong reference method for evaluating the effectiveness of AI-assisted MPPT.

3.4 AI-assisted MPPT formulation

In this work, MPPT is formulated as a supervised regression support task rather than a direct control problem. The ANN is trained to estimate the optimal PV operating voltage V_{MPP}based on measurable environmental inputs. Importantly, the ANN does not generate duty-cycle commands directly. The deployed ANN uses five environmental inputs, $[G_1, G_2, G_3, G_4, T]$, and predicts the array-level V_{MPP}. A toolbox-free multilayer perceptron with architecture $5-24-24-1$ was trained offline using ReLU hidden activations, a linear output layer, mean squared error (MSE) loss, and Adam optimization with a learning rate 10^{-3}, batch size 256, a maximum of 160 epochs, early stopping with patience 15, and train/validation/test splitting with train-only z-score normalization. The predicted $V_{MPP}$is supplied as the reference for the conventional PI voltage controller, which regulates the PV terminal voltage by adjusting the boost converter duty cycle. In this way, actuator-level decisions remain governed by classical control laws, while the AI component serves only as an aid to estimation. The resulting AI-assisted MPPT is therefore a hybrid structure in which machine learning augments, rather than replaces, conventional control.

3.5 Dataset generation and training

The ANN dataset was generated offline from the implemented PV model by sweeping irradiance and temperature over the operating range used in the study. Uniform-condition samples were generated for G= 200 to 1000w/m², and T=25⁰C to 45⁰C, additional partial-shading samples were generated using four-module irradiance vectors to represent mismatched operating conditions. For each operating point, the full P-V curve was evaluated and the target V_{MPP} label was obtained from the global maximum of the computed power curve. The input features were normalized using training-set z-score statistics only, and zero-mean Gaussian measurement noise was added during training to improve robustness. The dataset was then divided into training, validation, and test subsets for offline supervised learning. From an online-computation viewpoint, P&O has the lowest complexity because it only updates power differences and perturbs the duty ratio once per MPPT cycle.

Incremental Conductance is slightly more demanding because it computes filtered voltage and current increments and evaluates the incremental-conductance condition. The AI-assisted method incurs the highest online cost because each MPPT update requires a forward pass through a 5-24-24-1 MLP with 769 trainable parameters. Although this is still lightweight for software execution, it is computationally heavier than the classical benchmarks and therefore requires more careful real-time integration.

4. Simulation setup and test scenarios

This section presents the discrete-time simulation framework used to benchmark the MPPT strategies in MATLAB. The use of identical plant models, controller structure, and numerical settings ensures a fair comparison, while the imposed irradiance, temperature, and partial-shading profiles allow evaluation of dynamic behavior under representative operating conditions. Tracking efficiency, power ripple, and harvested energy are used to quantify the accuracy, stability, and robustness of each MPPT method. The overall benchmarking workflow is illustrated in Figure 2.

4.1 Simulation Environment

The simulation was performed using MATLAB R2025b with a fixed-step discrete solver that implements forward Euler integration. The fundamental sample time was $T_s = 100\ \mu s$, and the MPPT supervisory layer executed every 1 ms (10 plant steps). The photovoltaic (PV) array, DC-DC boost converter, and corresponding control loops were modeled within a unified framework so that P&O, Incremental Conductance (IncCond), and the AI-assisted MPPT strategy operated on the same plant model, numerical configuration, and simulation environment. This ensured objective and reproducible benchmarking. The PV array was modeled using a datasheet-based formulation representative of a 1 kW-class system, while the power-conditioning stage was represented by an averaged boost converter operating in continuous conduction mode.

A fixed-step discrete-time implementation was adopted, with plant-state updates at Ts = 100 µs, MPPT execution at TMPPT = 1 ms, and forward-Euler discretization applied to the averaged converter model. Thus, the supervisory ANN/MPPT layer operates at a rate that is 10 × slower than the plant-state update, which is consistent with the practical separation between fast converter dynamics and slower supervisory decision-making. The instantaneous PV output power used by all MPPT algorithms is defined as:

$$P_{pv}(k) = V_{pv}(k) I_{pv}(k) \tag{8}$$

Converter operation is regulated through the duty cycle generated by the inner PI voltage controller. The main electrical, control, and numerical parameters used throughout the simulations are summarized in Table 2 and were kept constant across all test cases to ensure fair comparison.

4.2 Test scenario

All MPPT methods were evaluated under identical benchmark profiles to ensure a fair comparison of dynamic tracking, robustness, and energy-harvesting performance. Three main scenarios were considered. First, a uniform-condition step test was used to examine transient tracking after abrupt irradiance changes. In this case, all four series-connected modules were subjected to the same irradiance profile, with step changes applied over time while the controller response and convergence behavior were recorded. Second, a fast-fluctuation test was used to emulate rapid cloud-induced variations by applying a square-wave irradiance profile of $1000 - 400\ W/m^2$ with a period of $0.2\ s$ at 25⁰C. Third, partial-shading conditions were introduced for the 4-series, 1-string array using unequal module irradiance vectors $[900, 900, 900, 900]$, $[900, 500, 300, 900]$, and $[700, 700, 250, 400]\mathrm{W/m^2}$, which generated multi-peak P-V characteristics. No explicit bypass-diode model was included.

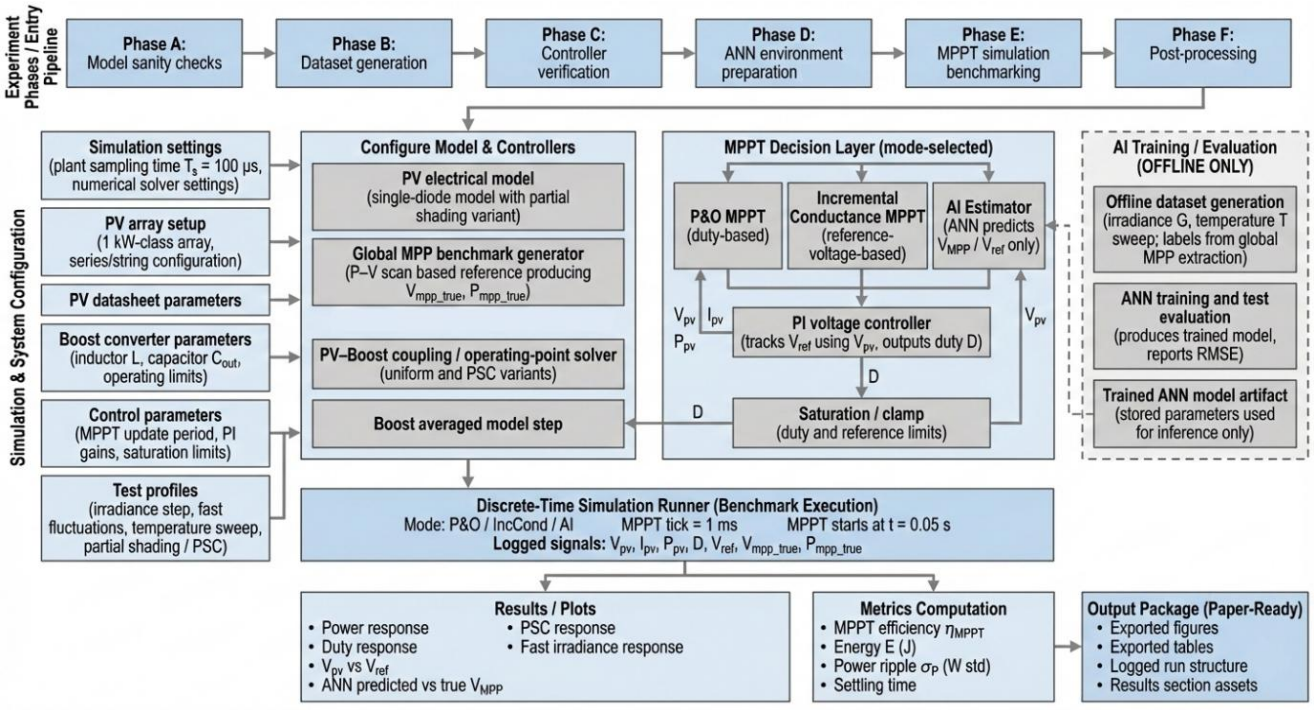

Figure 2. Block diagram of the AI-assisted MPPT benchmarking framework and simulation workflow

Table 2. Key simulation parameters

Parameter	Symbol	Value
PV rated power	P_{rated}	1 kW
PV configuration	-	4 series × 1 string
Inductor	L	2 mH
Output capacitor	C	1000μ F
Plant sampling time	T_s	100μ s
MPPT update period	T_{MPPT}	1 ms
Discretization method	-	Forward-Euler
Duty cycle limits	$D_{\min}$, $D_{\max}$	0.05, 0.95

These scenarios were selected to test steady operation, rapid environmental variation, and nonuniform operating conditions within the same simulation framework. For fair and reproducible benchmarking, all MPPT methods were evaluated using the same PV array and averaged boost-converter models, identical initial conditions, the same duty-cycle limits, identical plant and MPPT sampling settings, and the same environmental test profiles. For the AI-assisted and Incremental Conductance cases, the same inner PI voltage-control structure was retained to ensure the comparison reflects differences in MPPT decision logic rather than changes in plant- or actuator-level control.

4.3 Performance metrics

MPPT performance was evaluated using tracking efficiency, power ripple, and harvested energy. Tracking efficiency is defined as:

$$\eta_{MPPT} = \frac{\int_0^T P_{pv}(t)\,dt}{\int_0^T P_{mpp}(t)\,dt} \times 100 \quad (9)$$

where $\eta_{MPPT}$is expressed in %, $P_{pv}(t)$is the actual PV power in W, and $P_{mpp}(t)$is the theoretical maximum PV power in W. The harvested energy is computed as:

$$E = \int_0^T P_{pv}\,(t)\,dt \quad (10)$$

where $E$is expressed in joules (J). Power ripple is quantified using the standard deviation of sampled PV power over the evaluation interval:

$$\sigma_P = \sqrt{\frac{1}{N}\sum_{k=1}^{N}\left(P_{pv}(k) - \bar{P}_{pv}\right)^2} \quad (11)$$

where $\sigma_P$is in watts (W), $N$is the number of samples, and $\bar{P}_{pv}$is the mean PV power over the same interval.

5. Results

This section provides a comparative study of three MPPT approaches, Perturb and Observe (P&O), Incremental Conductance (IncCond), and the proposed AI-assisted MPPT with the same system models, numerical configurations, and test scenarios. The analysis examines the behavior of dynamic tracking, steady-state operation, energy harvesting, and the ability to withstand rapid irradiance changes and partial shading. All results are derived based on the simulation framework described in Section 4.

5.1 Dynamic tracking performance under uniform irradiance step

The transient response of the MPPT algorithms is first assessed under a uniform irradiance step from 1000 W/m² to 600 W/m² at t=1s, while keeping the temperature constant at 25 degC. The resultant PV output power trajectories for the classical MPPT controllers are given in Figure 3. It can be seen from Figure 3 that Incremental Conductance converges quickly to the new operating point after the change in irradiance, and operates near the theoretical maximum power with small oscillations. By comparison, the P&O approach also exhibits continuous swings around the peak power output due to its perturbation-based tracking mechanism. To investigate the internal control behavior responsible for this difference, the duty-cycle response of the Incremental Conductance controller during the same irradiance step test is shown in Figure 4.

Figure 4 shows that duty cycle is quickly stabilized after the irradiance transition, which implies good slope-based regulation and stable operating point enforcement. For comparison, the duty-cycle evolution of the P&O controller under the same conditions is also shown in Figure 5. Unlike Incremental Conductance, Figure 5 illustrates continuous duty-cycle oscillations even after the steady state is reached, which are a direct contributor to the steady-state power ripple. The quantitative tracking performance for this irradiance-step scenario is summarized in Table 3.

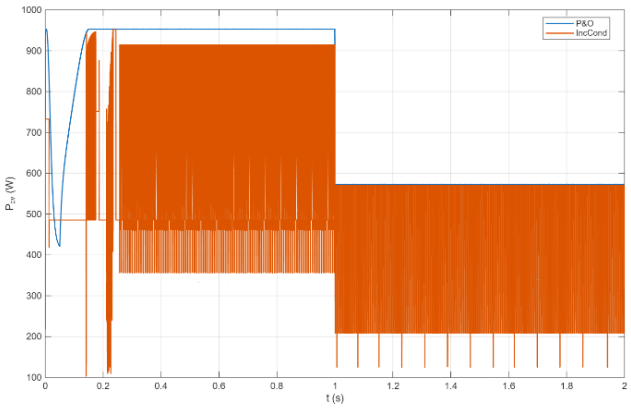

Figure 3. PV power comparison for P&O and Incremental Conductance under a uniform irradiance step (1000 → 600 W/m² at t = 1s, T = 25°C)

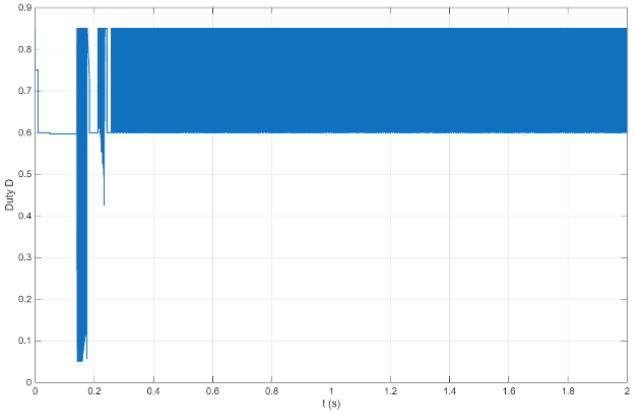

Figure 4. Duty-cycle response of Incremental Conductance under a uniform irradiance step

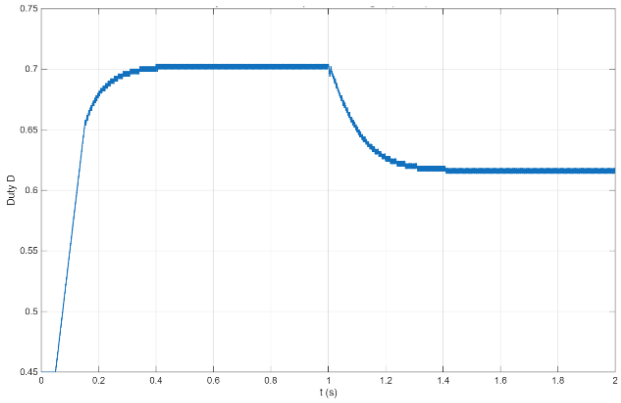

Figure 5. Duty-cycle response of P&O under a uniform irradiance step

Table 3. Dynamic tracking performance metrics under uniform irradiance step

MPPT Method	Tracking Efficiency (%)	Energy (J)	Settling Time (s)	Power Ripple (W, std)
P&O	98.13	1425.68	0.0010	0.0956
IncCond	99.89	1451.28	0.0037	0.0014
AI-assisted	67.92	986.80	0.9999	254.92

5.2 Steady-state tracking accuracy

Stability of the tracking is determined by considering the average PV power output and the power ripple after a complete steady state is achieved under constant irradiance conditions. The corresponding steady-state performance metrics for all MPPT strategies are summarized in Table 4. Incremental Conductance reaches the mean PV power of 744.21 W, which is almost the same as the theoretical maximum value of 745 W, with negligible ripple. The P&O technique operates slightly below the peak power operating point and exhibits higher ripple due to continuous perturbation. On the contrary, the AI-assisted MPPT operates far from the optimal operating point, resulting in lower mean power and much more severe ripple. These results show that accurate voltage reference estimation alone is insufficient without good closed-loop regulation.

5.3 ANN prediction characteristics

The standalone predictive capability of the ANN-based estimator is evaluated by comparing predicted and true maximum power point voltages on an unseen test set. The scatter plot of the prediction is given in Figure 6. Figure 6 shows that the ANN captures the general nonlinear mapping between operating conditions and optimal PV voltage, but its prediction accuracy remains limited for closed-loop MPPT use. On the unseen test set, the deployed model achieved an RMSE of 5.85 V, an MAE of 2.50 V, and a maximum absolute error of 41.66 V. Although the average error is moderate, occasional large voltage-reference errors can move the operating point away from the true MPP, especially during rapid irradiance changes and under partial shading. This explains why acceptable regression accuracy does not automatically translate into strong closed-loop MPPT performance.

Table 4. Steady-state tracking efficiency, harvested energy, and ripple under uniform conditions

MPPT Method	Mean (P_{MPP}) (W)	Mean (P_{pv}) (W)	Power Ripple Std (W)
P&O	745.00	731.08	0.0956
IncCond	745.00	744.21	0.0014
AI-assisted	745.00	506.02	254.92

5.4 Partial shading performance

The robustness of the MPPT strategies under partial shading is analyzed using stepwise shading profiles that introduce several local maxima in the PV power-voltage characteristic. The resulting PV power responses are given in Figure 7. It is apparent from Figure 7 that the classical MPPT methods exhibit greater robustness in partial shading. Both P&O and Incremental Conductance can keep the operation closer to the global maximum power point, whereas the AI-assisted MPPT exhibits significant power oscillations and fails to stabilize at a near-optimal operating point. The quantitative performance parameters for the partial-shading situation are summarized in Table 5.

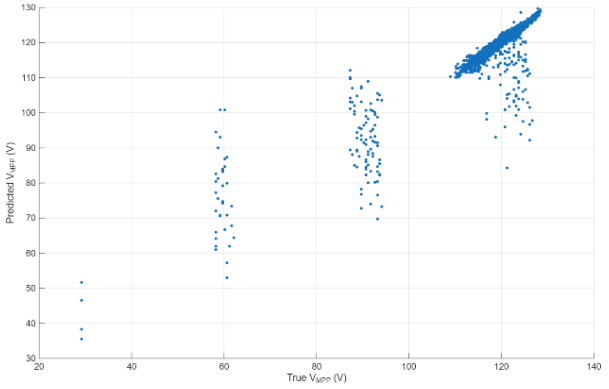

Figure 6 Predicted versus true $\mathbf{V_{MPP}}$ for the ANN estimator (test dataset, RMSE = 5.85 V)

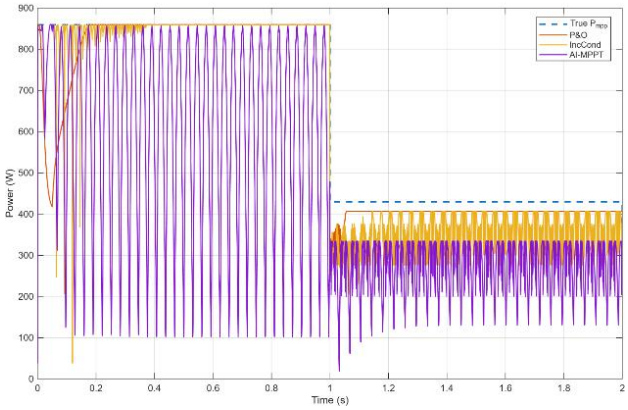

Figure 7. PV power comparison of P&O, Incremental Conductance, and AI-assisted MPPT under partial shading conditions

Table 5. Energy harvesting and ripple metrics under partial shading conditions

Profile	MPPT Method	Tracking Efficiency (%)	Energy (J)	Power Ripple Std (W)
PSC	P&O	96.21	1198.81	0.0937
PSC	IncCond	92.99	1158.73	0.3754
PSC	AI-assisted	67.84	845.32	235.58

5.5 Voltage regulation under partial shading

To further study the closed-loop voltage regulation behavior, Incremental Conductance and AI-assisted MPPT PV Terminal Voltage and Reference Voltage trajectories under partial shading are compared in Figure 8. Figure 8 shows that the Incremental Conductance is very close to the PV voltage and the reference voltage, whereas the AI-assisted MPPT exhibits greater deviations and oscillations after shading transitions. This action highlights how the sensitivity of an AI-assisted framework to estimation uncertainty becomes critical when it operates under nonuniform conditions.

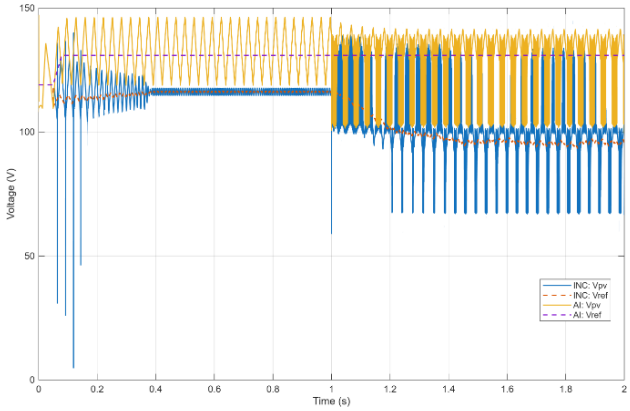

Figure 8. Comparison of PV voltage and reference voltage for Incremental Conductance and AI-assisted MPPT under partial shading

5.6 Performance under fast irradiance fluctuations

The response of the MPPT controllers to rapidly changing environmental conditions is analyzed based on a fast irradiance fluctuation profile (1000-400 W/m², period 0.2 s). PV power responses are the corresponding responses for Figure 9. Figure 9 shows that both P&O and Incremental Conductance exhibit significant power oscillations under rapid power fluctuations. However, Incremental Conductance exhibits a more structured, repeatable response, whereas P&O shows irregular oscillations that depend on the perturbation mechanism. The harvested energy and the ripple metrics for this scenario are summarized in Table 6.

5.7 Consolidated performance comparison

A consolidated comparison over all the evaluated scenarios, i.e., uniform irradiance, fast irradiance fluctuations, and partial shading, is presented in Table 7. It confirms that Incremental Conductance always yields the best balance among tracking efficiency, stability, and energy yield. P&O remains competitive in energy capture but is plagued by persistent oscillations. The intelligent MPPT, assisted by AI, highlights an important integration challenge in real-time dynamics and complex operating conditions. Overall, the results show that AI-assisted MPPT should be considered a support estimation framework rather than a replacement for classical MPPT algorithms. The results highlight the necessity of control-based integration and strict benchmarking for integrating machine learning into real-time photovoltaic control systems.

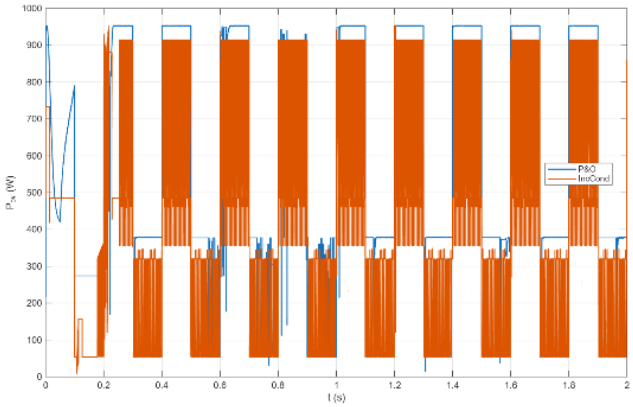

Figure 9. PV power comparison under fast irradiance fluctuations (1000 ↔ 400 W/m², period 0.2 s)

Table 6. Energy and ripple performance under fast irradiance fluctuations

MPPT Method	Energy (J)	Average Power (W)	Power Ripple Std (W)
P&O	1171.27	600.62	306.45
IncCond	898.77	460.88	312.71

Table 7. Summary of MPPT performance metrics across all test scenarios

Scenario	MPPT Method	Tracking Efficiency (%)	Energy (J)	Mean Power (W)	Power Ripple Std (W)
Uniform	P&O	98.13	1425.68	731.08	0.0956
Uniform	IncCond	99.89	1451.28	744.21	0.0014
Uniform	AI-assisted	67.92	986.80	506.02	254.92
PSC	P&O	96.21	1198.81	614.74	0.0937
PSC	IncCond	92.99	1158.73	594.19	0.3754
PSC	AI-assisted	67.84	845.32	433.48	235.58

6. Discussion

The aim of this work was not to present artificial intelligence as a replacement for classical MPPT algorithms, but to evaluate machine learning as a supporting estimator within a control-oriented MPPT framework. The results show that overall MPPT performance depends more on control integration, dynamic interaction, and robustness to changing operating conditions than on prediction accuracy alone. Among the tested methods, Incremental Conductance (IncCond) delivered the most stable and accurate tracking

under both uniform and partial-shading conditions because its slope-based logic enables fast and well-directed corrective action. In contrast, P&O remained simple and computationally efficient, but its perturbation mechanism caused persistent steady-state oscillations and higher power ripple. The AI-assisted MPPT framework in this work preserves a classical control hierarchy, where the ANN only estimates $V_{MPP}$and the inner PI loop enforces the reference through the boost converter. The ANN test error is moderate on average (RMSE 5.85 V, MAE 2.50 V), but the maximum error reaches 41.66 V, which is large enough to produce substantial off-MPP operation. This effect is amplified by the multi-rate implementation, because the ANN/MPPT layer updates at 1ms while the plant is updated at $100\mu s$. Under rapid irradiance changes or partial shading, this slower supervisory update can delay reference correction, and offline training further limits generalization in multi-peak operating regions. As a result, the controller may track a delayed or biased voltage reference, leading to lower harvested energy and greater power ripple than with Incremental Conductance.

These observations are consistent with prior work on AI-based MPPT. Dounis et al. [16] showed that adaptive neural control can improve PV tracking, while Mellit et al. [17] highlighted the broader potential of artificial intelligence in photovoltaic optimization. Liu et al. [18] reported that neural-network-based MPPT can perform well under fast-changing conditions, and Kofinas et al. [19] showed that reinforcement learning can support MPPT decision-making. Fathi and Parian [20] further demonstrated that hybrid intelligent methods can enhance tracking performance, while Roy et al. [21] indicated that deep learning can improve MPPT when trained on representative data. Taken together, these studies suggest that AI-based MPPT performance depends not only on prediction capability but also on control integration, timing, and generalization to operating conditions. Overall, the results made AI-assisted MPPT a useful research and design tool and not a panacea. The study highlights that successful MPPT depends less on prediction quality than on control integration and temporal alignment, and that traditional algorithms such as Incremental Conductance can serve as an effective baseline for operating photovoltaic systems in real time.

7. Conclusion

This work presented control-oriented benchmarking research on maximum power point tracking strategies for photovoltaic systems, with a specific focus on the role of machine learning when integrated into classical control architectures. Using a unified simulation framework for the entire power control system in MATLAB's discrete-time domain, namely Perturb and Observe, Incremental Conductance, and an AI-assisted MPPT scheme, was tested under identical conditions of dynamic irradiance, fast fluctuations, and partial shading. The results clearly show that Incremental Conductance is still a very good and reliable baseline for real-time MPPT. Its slope-based formulation allows for accurate directional tracking, low steady-state ripple, and robust operation across a wide range of operating conditions. In contrast, while the AI-assisted MPPT can successfully estimate the general trend of the optimal operating voltage, its closed-loop performance is strongly affected by estimation delays, reference uncertainty, and interactions with the inner PI voltage controller. The effects of this are limitations in its effectiveness under rapid transients and nonuniform conditions. The contribution of this study is methodological in terms of a fair and transparent benchmarking framework; analytical in terms of the interaction mechanisms governing the performance of AI-assisted MPPT; and cautionary in terms of demonstrating that prediction accuracy is not automatically translated into better control performance. Importantly, the work positions AI as a supporting estimation tool rather than an alternative to established MPPT algorithms. Future research will focus on adaptive and online learning concepts, hardware-in-the-loop verification, and stability consciousness when incorporating AI into multi-timescale photovoltaic control systems.

Ethical issue

The authors are aware of and comply with best practices in publication ethics, specifically regarding authorship (avoidance of guest authorship), dual submission, manipulation of figures, competing interests, and compliance with research ethics policies. The authors adhere to publication requirements that the submitted work is original and has not been published elsewhere.

Data availability statement

The manuscript contains all the data. However, additional data will be provided by the corresponding author upon reasonable request.

Conflict of interest

The authors declare no potential conflict of interest.

References

[1] M. L. Hoang, M. Mongilli, G. Matrella, and P. Ciampolini, “Artificial intelligence prediction of maximum power point tracking voltage and current based on battery for sensor reduction and complexity minimization for photovoltaic charge controller,” e-Prime – Advances in Electrical Engineering, Electronics and Energy, vol. 5, p. 101110, 2025. doi: 10.1016/j.prime.2025.101110.

[2] Ž. Zečević and M. Rolevski, “Neural network approach to MPPT control and irradiance estimation,” Appl. Sci., vol. 10, no. 15, p. 5051, 2020. doi: 10.3390/app10155051.

[3] Y. Du, K. Yan, Z. Ren, and W. Xiao, “Designing localized MPPT for PV systems using fuzzy-weighted extreme learning machine,” Energies, vol. 11, no. 10, p. 2615, 2018. doi: 10.3390/en11102615.

[4] K. Y. Chou, S. T. Yang, and Y. P. Chen, “Maximum power point tracking of photovoltaic system based on reinforcement learning,” Sensors, vol. 19, no. 22, p. 5054, 2019. doi: 10.3390/s19225054.

[5] M. J. Khan and L. Mathew, “Artificial neural network-based maximum power point tracking controller for real-time hybrid renewable energy system,” Soft Comput., vol. 25, no. 8, pp. 6557–6575, 2021. doi: 10.1007/s00500-021-05653-0.

[6] Z. Xie and Z. Wu, “Maximum power point tracking algorithm of PV system based on irradiance estimation and multi kernel extreme learning machine,” Sustain. Energy Technol. Assessments, vol. 44, p. 101090, 2021. doi: 10.1016/j.seta.2021.101090.

[7] H. Bouaouaou, D. Lalili, and N. Boudjerda, “Model predictive control and ANN-based MPPT for a multi-level grid-connected photovoltaic inverter,” Electr.

Eng., vol. 104, no. 3, pp. 1229–1246, 2022. doi: 10.1007/s00202-021-01355-w.

[8] L. Avila, M. De Paula, M. Trimboli, and I. Carlucho, "Deep reinforcement learning approach for MPPT control of partially shaded PV systems in smart grids," Appl. Soft Comput., vol. 97, p. 106711, 2020. doi: 10.1016/j.asoc.2020.106711.

[9] L. F. Giraldo, J. F. Gaviria, M. I. Torres, C. Alonso, and M. Bressan, "Deep reinforcement learning using deep Q network for global maximum power point tracking: Design and experiments in real photovoltaic systems," Heliyon, vol. 10, no. 21, p. e37974, 2024. doi: 10.1016/j.heliyon.2024.e37974.

[10] A. Wadehra, S. Bhalla, V. Jaiswal, K. P. S. Rana, and V. Kumar, "A deep recurrent reinforcement learning approach for enhanced MPPT in PV systems," Appl. Soft Comput., vol. 162, p. 111728, 2024. doi: 10.1016/j.asoc.2024.111728.

[11] L. Yin, J. Li, N. Wang, and F. Gao, "Deep predictive data representation model control for photovoltaic maximum power point tracking under partial shading conditions," Energy Convers. Manag., vol. 322, p. 119171, 2024. doi: 10.1016/j.enconman.2024.119171.

[12] S. Danyali, M. Babaeifard, M. Shirkhani, A. Azizi, J. Tavoosi, and Z. Dadvand, "A new neuro-fuzzy controller based maximum power point tracking for a partially shaded grid-connected photovoltaic system," Heliyon, vol. 10, no. 17, p. e36747, 2024. doi: 10.1016/j.heliyon.2024.e36747.

[13] H. Wang, L. Li, H. Ye, and W. Zhao, "Enhancing MPPT efficiency in PV systems under partial shading: A hybrid POA & PO approach for rapid and accurate energy harvesting," Int. J. Electr. Power Energy Syst., vol. 162, p. 110260, 2024. doi: 10.1016/j.ijepes.2024.110260.

[14] K. Chnini, M. Abdou Tankari, H. Jouini, H. Allagui, M. A. Ibrahim, and E. Touti, "Embedded processor-in-the-loop implementation of ANFIS-based nonlinear MPPT strategies for photovoltaic systems," Energies, vol. 18, no. 10, p. 2470, 2025. doi: 10.3390/en18102470.

[15] A. Satpathy, N. Nayak, N. Hannon, and N. N. Ali, "A new real-time maximum power point tracking scheme for PV based microgrid stability using online deep ridge extreme learning machine algorithm," Results Eng., vol. 20, p. 101590, 2023. doi: 10.1016/j.rineng.2023.101590.

[16] A. I. Dounis, P. Kofinas, G. Papadakis, and C. Alafodimos, "A direct adaptive neural control for maximum power point tracking of photovoltaic system," Sol. Energy, vol. 115, pp. 145–165, 2015. doi: 10.1016/j.solener.2015.02.004.

[17] A. Mellit, S. A. Kalogirou, L. Hontoria, and S. Shaari, "Artificial intelligence techniques for sizing photovoltaic systems: A review," Renew. Sustain. Energy Rev., vol. 13, no. 2, pp. 406–419, 2009. doi: 10.1016/j.rser.2008.01.006.

[18] Y. H. Liu, C. L. Liu, J. W. Huang, and J. H. Chen, "Neural-network-based maximum power point tracking methods for photovoltaic systems operating under fast changing environments," Sol. Energy, vol. 89, pp. 42–53, 2013. doi: 10.1016/j.solener.2012.11.017.

[19] P. Kofinas, S. Doltsinis, A. I. Dounis, and G. A. Vouros, "A reinforcement learning approach for MPPT control method of photovoltaic sources," Renew. Energy, vol. 108, pp. 461–473, 2017. doi: 10.1016/j.renene.2017.03.008.

[20] M. Fathi and J. A. Parian, "Intelligent MPPT for photovoltaic panels using a novel fuzzy logic and artificial neural networks based on evolutionary algorithms," Energy Rep., vol. 7, pp. 1338–1348, 2021. doi: 10.1016/j.egyr.2021.02.051.

[21] B. Roy, S. Adhikari, S. Datta, K. J. Devi, A. D. Devi, and T. S. Ustun, "Harnessing deep learning for enhanced MPPT in solar PV systems: An LSTM approach using real-world data," Electricity, vol. 5, no. 4, pp. 843–860, 2024. doi: 10.3390/electricity5040042.